

## RESEARCH ARTICLE

# STAC3 variants cause a congenital myopathy with distinctive dysmorphic features and malignant hyperthermia susceptibility

Irina T. Zaharieva<sup>1</sup>  | Anna Sarkozy<sup>1,2</sup> | Pinki Munot<sup>1,2</sup> | Adnan Manzur<sup>1,2</sup> | Gina O'Grady<sup>3,4</sup> | John Rendu<sup>5</sup> | Eduardo Malfatti<sup>6</sup> | Helge Amthor<sup>7,8</sup> | Laurent Servais<sup>9</sup> | J. Andoni Urtizbera<sup>10</sup> | Osorio Abath Neto<sup>11,12</sup> | Edmar Zanoteli<sup>11</sup> | Sandra Donkervoort<sup>12</sup> | Juliet Taylor<sup>13</sup> | Joanne Dixon<sup>14</sup> | Gemma Poke<sup>15</sup> | A. Reghan Foley<sup>12</sup> | Chris Holmes<sup>2</sup> | Glyn Williams<sup>2</sup> | Muriel Holder<sup>16</sup> | Sabrina Yum<sup>17</sup> | Livija Medne<sup>18</sup> | Susana Quijano-Roy<sup>8,19</sup> | Norma B. Romero<sup>6</sup> | Julien Fauré<sup>5</sup> | Lucy Feng<sup>1</sup> | Laila Bastaki<sup>20</sup> | Mark R. Davis<sup>21</sup> | Rahul Phadke<sup>1,2</sup> | Caroline A. Sewry<sup>1,22</sup> | Carsten G. Bönnemann<sup>12</sup> | Heinz Jungbluth<sup>23,24,25</sup> | Christoph Bachmann<sup>25</sup> | Susan Treves<sup>25,26</sup> | Francesco Muntoni<sup>1,2,27</sup>

<sup>1</sup>Dubowitz Neuromuscular Centre, UCL Great Ormond Street Institute of Child Health, London, UK

<sup>2</sup>Great Ormond Street Hospital, London, UK

<sup>3</sup>Institute of Neuroscience and Muscle Research, Children's Hospital at Westmead, Sydney, New South Wales, Australia

<sup>4</sup>Discipline of Paediatrics and Child Health Clinical School, University of Sydney, Sydney, New South Wales, Australia

<sup>5</sup>UFR de Médecine, Centre Hospitalier Universitaire Grenoble Alpes, Université Grenoble Alpes, Grenoble, France

<sup>6</sup>Neuromuscular Morphology Unit and Neuromuscular Pathology Reference Center Paris-Est, Center for Research in Myology, Groupe Hospitalier Universitaire La Pitié-Salpêtrière, Paris, France

<sup>7</sup>UFR des sciences de la santé, Versailles Saint-Quentin-en-Yvelines University, Montigny-le-Bretonneux, France

<sup>8</sup>Service de Pédiatrie, Centre Hospitalier Universitaire Raymond Poincaré, Garches, France

<sup>9</sup>Institut I-Motion, Hôpital Armand Trousseau, Paris, France

<sup>10</sup>Centre de Compétence Neuromusculaire, FILNEMUS, Hôpital Marin, Hendaye, France

<sup>11</sup>Departamento de Neurologia, Faculdade de Medicina da Universidade de São Paulo (FMUSP), São Paulo, Brazil

<sup>12</sup>Neuromuscular and Neurogenetic Disorders of Childhood Section, National Institutes of Health, Bethesda, Maryland, USA

<sup>13</sup>Genetic Health Service New Zealand, Auckland, New Zealand

<sup>14</sup>Genetic Health Service New Zealand, Christchurch, New Zealand

<sup>15</sup>Genetic Health Service New Zealand, Wellington, New Zealand

<sup>16</sup>Department of Clinical Genetics, Guy's Hospital, London, UK

<sup>17</sup>Division of Neurology, The Children's Hospital of Philadelphia, Philadelphia, Pennsylvania

<sup>18</sup>Division of Human Genetics, The Children's Hospital of Philadelphia, Philadelphia, Pennsylvania

<sup>19</sup>Centre de Référence Neuromusculaire GNMH, FILNEMUS, Université de Versailles, Versailles, France

<sup>20</sup>Kuwait Medical Genetics Centre, Maternity Hospital, Kuwait City, Kuwait

<sup>21</sup>Department of Diagnostic Genomics, Pathwest Laboratory Medicine, QEII Medical Centre, Nedlands, Western Australia, Australia

<sup>22</sup>Wolfson Centre for Inherited Neuromuscular Diseases, RJA Orthopaedic Hospital, Oswestry, UK

<sup>23</sup>Randall Division for Cell and Molecular Biophysics, Muscle Signaling Section, King's College London, London, UK

<sup>24</sup>Department of Basic and Clinical Neuroscience, IoPPN, King's College London, London, UK

<sup>25</sup>Department of Anesthesia and Biomedicine, University Hospital Basel, Basel, Switzerland

<sup>26</sup>Department of Life Sciences, University of Ferrara, Ferrara, Italy

<sup>27</sup>NIHR Great Ormond Street Hospital Biomedical Research Centre, London, UK

#### Correspondence

Irina Zaharieva, Institute of Child Health, University College London, 30 Guilford Street, London WC1N 1EH, UK.

Email: i.zaharieva@ucl.ac.uk

#### Funding information

NeRAB Association; FP7 Health, Grant/Award Number: 2012-305121; NIHR Great Ormond Street Hospital Biomedical Research Centre; Horizon 2020 Framework Programme, Grant/Award Number: 779257; National Institute for Neurological Disorders and Stroke/NIH; Schweizerischer Nationalfonds zur Förderung der Wissenschaftlichen Forschung, Grant/Award Number: 31003A-169316; OPO Stiftung; Muscular Dystrophy Association, Grant/Award Number: MDA577346

Communicated by Madhuri Hegde

#### Abstract

SH3 and cysteine-rich domain-containing protein 3 (STAC3) is an essential component of the skeletal muscle excitation–contraction coupling (ECC) machinery, though its role and function are not yet completely understood.

Here, we report 18 patients carrying a homozygous p.(Trp284Ser) STAC3 variant in addition to a patient compound heterozygous for the p.(Trp284Ser) and a novel splice site change (c.997-1G > T). Clinical severity ranged from prenatal onset with severe features at birth, to a milder and slowly progressive congenital myopathy phenotype. A malignant hyperthermia (MH)-like reaction had occurred in several patients.

The functional analysis demonstrated impaired ECC. In particular, KCl-induced membrane depolarization resulted in significantly reduced sarcoplasmic reticulum Ca<sup>2+</sup> release. Co-immunoprecipitation of STAC3 with Ca<sub>v</sub>1.1 in patients and control muscle samples showed that the protein interaction between STAC3 and Ca<sub>v</sub>1.1 was not significantly affected by the STAC3 variants.

This study demonstrates that *STAC3* gene analysis should be included in the diagnostic work up of patients of any ethnicity presenting with congenital myopathy, in particular if a history of MH-like episodes is reported. While the precise pathomechanism remains to be elucidated, our functional characterization of *STAC3* variants revealed that defective ECC is not a result of Ca<sub>v</sub>1.1 sarcolemma mislocalization or impaired STAC3-Ca<sub>v</sub>1.1 interaction.

#### KEYWORDS

congenital myopathy, excitation–contraction coupling, malignant hyperthermia, STAC3

## 1 | INTRODUCTION

Excitation–contraction coupling (ECC) is a process in which consecutive events lead from the depolarization of the muscle fiber membrane to increased cytosolic Ca<sup>2+</sup> release and initiation of muscle contraction. ECC occurs at specialized structures, termed triads, composed of a T-tubule and two lateral sacs of sarcoplasmic reticulum. The two major components of the ECC protein complex are the L-type voltage-sensitive Ca<sup>2+</sup> channel (DHPR) and the sarcoplasmic reticulum Ca<sup>2+</sup> release channel RyR1 (Rios & Pizarro, 1991). Although the role of DHPR and RyR1 in ECC has been extensively investigated, the precise regulatory mechanism underlying the mechanical coupling in skeletal muscle ECC and whether additional protein components are required is currently not entirely understood.

SH3 and cysteine-rich domain-containing protein 3 (STAC3; MIM# 615521) is essential for muscle contraction by facilitating ECC through a not completely understood mechanism (Horstick et al., 2013; Nelson et al., 2013). STAC3 (Uniprot# Q96MF2) is specifically expressed in skeletal muscle (Bower et al., 2012; Horstick et al., 2013; Reinholt, Ge, Cong, Gerrard, & Jiang, 2013), it is localized to the triads (Horstick et al., 2013; Nelson et al., 2013), and interacts with RyR1 and the DHPR complex (Horstick et al., 2013). More recently it was shown that STAC3 interacts with the Ca<sub>v</sub>1.1 II-III loop (Polster, Nelson, Papadopoulos, Olson, & Beam, 2018; Wong King Yuen, Campiglio, Tung, Flucher, & Van Petegem, 2017), a region previously identified as critical for the

conformational coupling with RyR1 and for skeletal muscle ECC (Grabner, Dirksen, Suda, & Beam, 1999; Nakai, Tanabe, Konno, Adams, & Beam, 1998).

The relevance of STAC3 in coupling the membrane depolarization to Ca<sup>2+</sup> release from the sarcoplasmic reticulum has been demonstrated using mouse and zebrafish models. Homozygous *Stac3* knockout mice (KO) are paralyzed and die shortly after birth due to hypoxia as a result of paralyzed respiratory muscles (Nelson et al., 2013), a phenotype similar to other animal models with disrupted ECC (Flucher, Phillips, & Powell, 1991; Nishi, 1995). The complete lack of *Stac3* in the spontaneous zebrafish mutant *mi34* led to an aberrant locomotor phenotype and lethality of fish at the larval stage (Horstick et al., 2013). Notably, the skeletal muscles from zebrafish and mouse *Stac3*-null animals displayed null (Nelson et al., 2013; Reinholt et al., 2013) or significantly reduced (Cong, Doering, Mazala, et al., 2016; Horstick et al., 2013) ability to contract following membrane depolarization. In the mutant animals neither the contractile apparatus nor RyR1 function appeared directly affected as addition of RyR1 agonists, such as 4-CMC or caffeine, were able to induce muscle contraction with similar force magnitude compared to the wild-type animals (Horstick et al., 2013; Nelson et al., 2013). Defects in the nervous system were also unlikely since tactile stimulation induced synaptic responses in the mutant *mi34* zebrafish (Horstick et al., 2013). These data indicated that the abolished ability of *stac3*-null muscles to contract in response

to depolarization was a result of defective ECC caused by the lack of Stac3.

The role of STAC3 in ECC has further been investigated in several recent studies. In heterologous cells (tsA201) Stac3 has been shown to be important for the trafficking of Ca<sub>v</sub>1.1 (the pore-forming subunit of DHPR) to the plasma membrane (Polster, Perni, Bichraoui, & Beam, 2015). Subsequent studies from the same group and others, however reported that in *Stac3* KO myotubes, the failure of ECC was not a result of a trafficking defect of Ca<sub>v</sub>1.1. Albeit at reduced levels, Ca<sub>v</sub>1.1 was present on the plasma membrane but was not able to generate ECC Ca<sup>2+</sup> currents (Linsley, Hsu, Wang, & Kuwada, 2017; Polster, Nelson, Olson, & Beam, 2016). The ECC was only restored after expression of the WT Stac3, demonstrating that Stac3 is important for the functional link between Ca<sub>v</sub>1.1 and RyR1 (Linsley, Hsu, Wang, et al., 2017; Polster et al., 2016).

The first report linking variants in *STAC3* to a human disorder described a homozygous missense *STAC3* variant p.(Trp284Ser) as causative for Native American myopathy (NAM; MIM# 255995; Horstick et al., 2013). NAM is an autosomal recessive disorder found in the Lumbee Indian population of North Carolina and characterized by congenital muscle weakness, delayed motor development, susceptibility to malignant hyperthermia (MH), multiple joint contractures, short stature, scoliosis, and distinctive facial features such as ptosis, palate abnormalities, and long and narrow face (Stamm et al., 2008). Recently, recessive variants in *STAC3* have been reported in patients with features overlapping Carey-Fineman-Ziter and Moebius syndrome (Grzybowski et al., 2017; Telegrafi et al., 2017).

Here, we describe 18 patients carrying *STAC3* pathogenic variants, the largest cohort of patients with *STAC3*-related congenital myopathy studied up to now. Importantly, the patients investigated here were not of Native American origin. Seventeen patients, of African, Middle Eastern, Afro-Caribbean, Comorian, and South American descent, carried the previously described homozygous NAM p.Trp284Ser *STAC3* variant and one patient, of African/Afro-Caribbean descent, was compound heterozygous for the NAM variant in one allele and a novel c.997-1G > T splice site variant in the other allele.

## 2 | MATERIALS AND METHODS

### 2.1 | Ethical approval

Informed consent was obtained from all patients or from their parents or legal guardians. The study was approved by the Health Research Authority, NRES Committee East of England--Hatfield (REC 13/EE/0398) and National Institute of Neurological Disorders and Stroke, National Institutes of Health (12-N-0095).

### 2.2 | Whole exome and Sanger sequencing

Whole exome sequencing (WES) was carried out in the probands from families PN1, PN3, PN9, PN10, and PN12. Targeted panel sequencing of known congenital myopathy genes was performed in the probands from families PN4, PN5, PN6, PN7, PN8, and PN11. Sanger sequencing

was used to identify the *STAC3* c.851G > C p.(Trp284Ser) variant in the affected cases from PN2.

Validation of the *STAC3* variants and segregation analysis in family members were carried out using Sanger sequencing.

The novel *STAC3* c.997-1G > T variant identified in PN5 has been submitted to Leiden Open Variation Database ([www.LOVD.nl/STAC3](http://www.LOVD.nl/STAC3))

### 2.3 | Muscle histology

Muscle biopsies, taken from cases PN2D, PN3A, PN4, PN5, PN7, PN8, and PN12, were processed using standard histochemical stains previously described (Dubowitz, Sewry, & Oldfors, 2013). Electron microscopic analyses were done in samples from cases PN5, PN7, and PN8.

### 2.4 | Muscle magnetic resonance imaging (MRI)

Muscle MRI of the lower limbs by conventional T1 weighted sequences was performed in patients PN1, PN2A, PN2B, and PN4.

### 2.5 | Immunofluorescent analysis

The primary antibodies used for the immunofluorescent analysis in cryosections from muscle biopsies were anti-RyR1 (ab2868, Abcam plc.) and anti-Cav1.1 (SC-8160, Santa Cruz, CA).

Confocal immunohistochemistry on myotubes was performed as previously described (Bachmann et al., 2017).

### 2.6 | Western blotting

Protein extracts (30 μg) from muscle biopsies were separated on pre-cast NuPAGE protein gels (Thermo Fisher Scientific, Waltham, MA) and transferred to nitrocellulose membranes. The primary antibodies used were anti-Ca<sub>v</sub>1.1 (sc-514685, Santa Cruz Biotechnology, Dallas, TX), anti-*STAC3* (20392-1-AP, Proteintech Group, Rosemont, IL), anti-DHPR-β<sub>1a</sub> (ab28502, Abcam, Cambridge, UK), and anti-α-actinin (D6F6, CST).

### 2.7 | Molecular modeling

The molecular modeling of the p.(Trp284Ser) *STAC3* was based on the nuclear magnetic resonance (NMR) structure of the first SH3 domain of Stac protein (Protein Data Bank accession code 2DL4). For the analysis of the effect of c.997-1G > T variant we used homology modeling of the *STAC3* tandem SH3 domains carrying the deleted IVVQ amino acids and the crystal structure of human *STAC1* tandem SH3 domains (6B25). The modeling was performed using Chimera visualization system (Pettersen et al., 2004) and Modeller (Sali & Blundell, 1993).

### 2.8 | Calcium measurements

Primary muscle cells were cultured as previously described (Bachmann et al., 2017; Censier, Urwyler, Zorzato, & Treves, 1998). Statistical analysis was performed using the Student's *t*-test for paired samples or using analysis of variance test (ANOVA) when more than two groups were compared. Origin computer program (Microcal Software, Inc., Northampton, MA) was used for statistical analysis and dose response

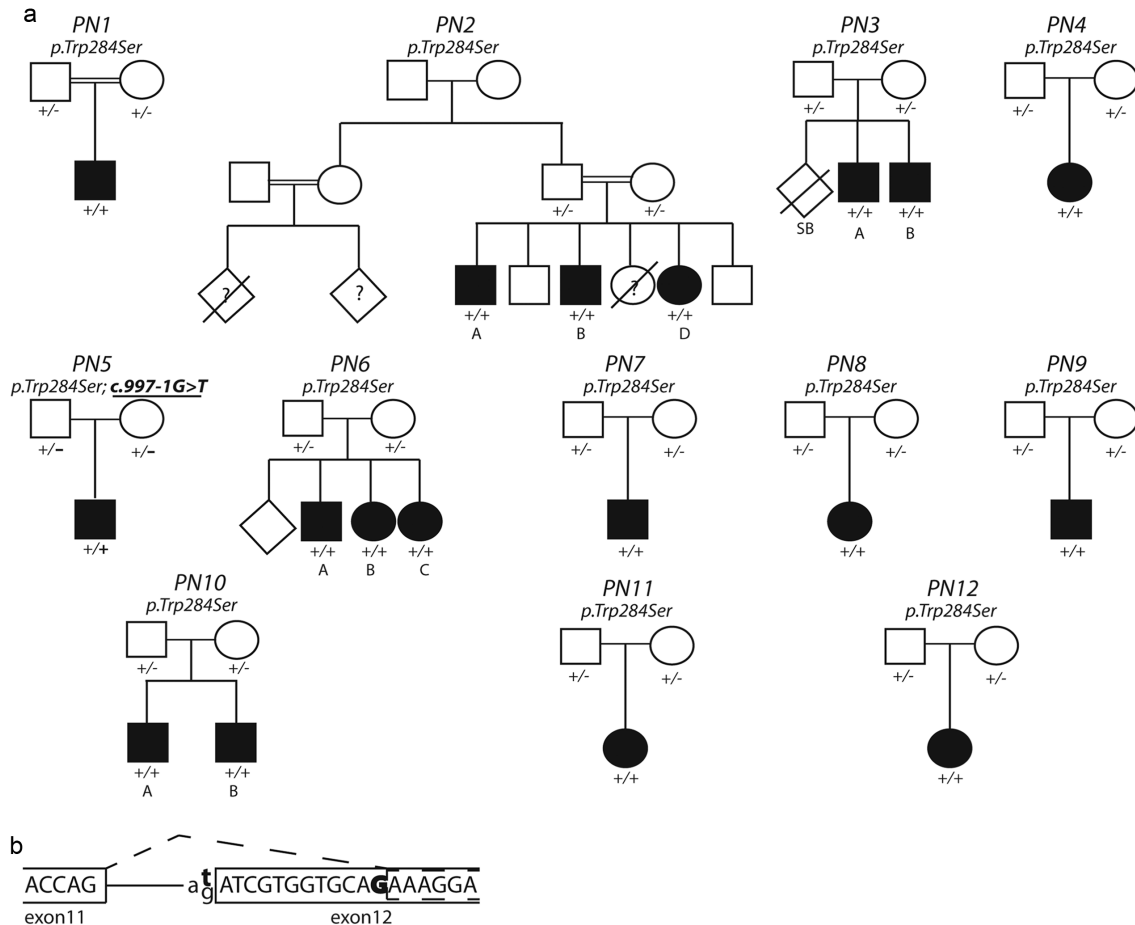


**FIGURE 1** Family trees of the *STAC3* patients described in the study and consequence of the *STAC3* c.997-1G > T variant. (a) Pedigrees of the *STAC3* families. Affected individuals are presented with shaded symbols. SB: stillbirth. (b) Schematic presentation of the consequence of the c.997-1G > T mutation. The aberrant splicing event is presented in bold and with a dotted line

curve generation. The  $EC_{50}$  and  $R_{max}$  values were calculated using the Origin program from sigmoidal curve fitting of all the data points.

## 2.9 | Co-immunoprecipitation

Protein extracts from muscle biopsies were solubilized and clarified. Antibodies against  $Ca_v1.1$  (sc-8160, Santa Cruz Biotechnology) or mouse IgG1 (GTX35014, GeneTex, Irvine, CA) were used. The solubilized muscle homogenates were incubated with Protein G-Sepharose and centrifuged. The bead pellets were loaded on an acrylamide gel, transferred onto nitrocellulose membrane and incubated with anti-*STAC3* antibody (20392-1-AP, Proteintech Group).

## 3 | RESULTS

### 3.1 | Identification of patients carrying *STAC3* variants

WES analysis in patient PN1 (Figure 1) revealed a homozygous c.851G > C, p.(Trp284Ser) variant in exon 10 of the *STAC3* gene (NM\_145064.2). Sanger sequencing of *STAC3* exon 10 or panel sequencing of known neuromuscular genes was carried out in cases PN2D, PN4, PN5, and PN6A, presenting with distinctive clinical fea-

tures similar to those noted in PN1. All patients, apart from PN5, carried the same homozygous missense c.851G > C, p.(Trp284Ser) *STAC3* variant. Compound heterozygous *STAC3* c.851G > C, p.(Trp284Ser) and an acceptor splice site c.997-1G > T variant was detected in PN5. The c.997-1G > T variant abolishes the acceptor splice site of the last exon of *STAC3* (exon 12), leading to activation of a cryptic acceptor site within exon 12 (Figure 1b). cDNA sequencing confirmed a deletion of 12 nucleotides from the mature *STAC3* RNA. This in-frame deletion eliminates four amino acids from the second *STAC3* SH3 domain.

We further identified seven families (Figure 1) with nine affected members carrying the homozygous *STAC3* c.851G > C p.(Trp284Ser) variant.

Sanger sequencing in additional affected and healthy family members confirmed the segregation of the *STAC3* variants with the disease following an autosomal recessive inheritance pattern. The families are apparently unrelated and of African, Afro-Caribbean, Comorian, Middle Eastern, or South American origin (Table 1).

### 3.2 | Clinical features of cohort members

Detailed clinical information was available for 18 patients (12 families) with confirmed *STAC3* variants (Table 1). A sister and two maternal cousins in family PN2 were affected by a similar condition but

**TABLE 1** Clinical characteristics of the patients with STAC3 variants

	PN1	PN2A	PN2B	PN2D	PN3A	PN3B	PN4	PN5	PN6A	PN6B	PN6C	PN7	PN8	PN9	PN10A	PN10B	PN11	PN12	
Gender	Male	Male	Male	Female	Male	Male	Female	Female	Male	Female	Female	Male	Female	Male	Male	Male	Female	Female	
Geographic origin	AF	ME	ME	ME	AF	AF	AC	AF/AC	AF	AF	AF	CO	AF	ME	ME	ME	AF	AF	
Age last seen (years)	16	20	14	9	9	5	23	2.2	12	4.5	2.5	3	0.5	13.8	14	13	2.9	5	
Prenatal features	↓FM	NR	NR	↓FM	-	-	-	Talipes, polyhydr- amnios	NR	-	Polyhydr- amnios	Polyhydr- amnios	-	Breech	NR	NR	IUGR, ↓FM	-	
<b>Features at birth and infancy</b>																			
Contractures	BT	BT	MT	BT	BT, camp- todactyly	Wrists	BT	Multiple contrac- tures, BT	-	Overri- ding toes	-	BT	-	Mild neck contrac- ture	BT, knee, campto- dactyly 5th finger, CHD	BT, knee, campto- dactyly 5th finger	BT, thumb	CHD, BT	
Hypotonia	+	NR	NR	NR	+	+	+	+	+	+	+	+	+	+	+	+	+	+	
Respiratory impairment	-	-	-	-	-	-	-	+	CPAP 48h	-	CPAP 48h, + oxygen for 3 weeks	+	+	-	+	+	CPAP 48h	-	
Feeding difficulties	+	NR	+	+	-	+	+	+	+	+	+	-	+	PEG	+	+	+	+	
Palate anomalies	-	CP	HP	CP	CP, HP	CP, HP	-	BU	-	-	-	-	-	HP	CP	HP	HP	HP	
Failure to thrive	+	+	+	+	+	+	-	+	-	-	+	+	-	+	-	+	+	-	
Further features at birth	Neck ptery- gium	NR	NR	↓BW	↓BW	↓BW	Elbow pterygium, elevated hemi- diaphragm	Elbow pterygium, elevated hemi- diaphragm	-	-	-	Facial weakness	↓BW, pre- maturity	HP	R	Inguinal hernia	↓BW	-	

(Continues)

**TABLE 1** (Continued)

	PN1	PN2A	PN2B	PN2D	PN3A	PN3B	PN4	PN5	PN6A	PN6B	PN6C	PN7	PN8	PN9	PN10A	PN10B	PN11	PN12		
<b>Clinical features at last assessment</b>																				
Motor delay	+	+	+	+	+	+	+	+	+	+	+	+	+	-	+	+	+	+	+	
Muscle weakness <sup>a</sup>	Facial, axial, proximal	+	Facial, axial, proximal	Facial, axial, proximal	Facial, neck, proximal, distal, UL, LL	Proximal	Facial, axial, proximal, UL, LL	Facial, axial, proximal, and distal LL	Facial, axial, proximal	Axial	Facial, axial	Axial, proximal	Axial, proximal, distal	Facial, proximal, distal	Mild distal	Mild distal	Facial, axial, proximal, distal	Facial, axial, proximal, LL	+	
Course of weakness	Static	NR	/	Static	Static	/	NR	/	/	/	/	/	NR	Static	Static	Static	Static	Static	Static	Static
Maximum motor ability	Short walk	Walk	Walk	Walk	Walk	Walk	Walk	TY	Walk	Walk	TY	Sit	TY	Run	Walk	Walk	Short walk	Walk	Walk	Walk
Muscle atrophy/ <sup>b</sup> wasting	+	+	+	UL and LL	Calves	Calves	Calves	Calves	-	-	-	Calves	-	+	+	+	-	-	-	-
Muscle tone	NR	NR	↓	↓	↓	↓	NR	↓	↓	↓	↓	↓	↓	↓	↓	↓	↓	↓	↓	↓
Contractures	Neck, spine, FF, thumb	Ankles	-	Spine, FF, ankles	FF, ankles	R ankle	Ankles	Elbow, FF, ankles	-	-	-	Ankles	Knees	Neck, wrist, FF	FF, ankle	FF, ankle	FF, ankle	FF, ankle	Hips, feet	Hips, feet
Joint hyperlaxity <sup>a</sup>	Elbows, knees, FF	NR	-	+	-	-	+	+	+	+	+	NR	NR	Thumbs	-	-	-	-	-	-
Scoliosis/kyphosis	K and S	K and S	S	K and S	-	K and S	K and S	K and S	-	-	K and S	S	-	+	S	S	-	-	-	-
Short stature	+	+	+	+	+	-	-	-	-	-	-	-	-	+	+	+	+	+	+	+
Facial features <sup>a</sup>	Ptosis, myopathic face	Ptosis, myopathic face	Ptosis, myopathic face	Ptosis, myopathic face	Ptosis, myopathic face	Ptosis, myopathic face	Ptosis, myopathic face	Ptosis, myopathic face	Ptosis, myopathic face	Ptosis, myopathic face	Ptosis, myopathic face	Ptosis, myopathic face	Ptosis, myopathic face	Ptosis, myopathic face	Ptosis, myopathic face	Ptosis, myopathic face	Ptosis, myopathic face	Ptosis, myopathic face	Ptosis, myopathic face	Ptosis, myopathic face

(Continues)

TABLE 1 (Continued)

	PN1	PN2A	PN2B	PN2D	PN3A	PN3B	PN4	PN5	PN6A	PN6B	PN6C	PN7	PN8	PN9	PN10A	PN10B	PN11	PN12
Dental problems	Malocclusion, prominent jaw	Caries, malar hypoplasia	Caries, malar hypoplasia	Malar hypoplasia	Crowded teeth	-	-	TY	-	-	-	Malocclusion, prominent jaw	TY	-	Maxillary hypoplasia	Maxillary hypoplasia	-	-
Feeding difficulties	+	+	+	+	PEG	+	-	PEG	+	+	+	PEG	+	-	-	-	+	-
Respiratory findings	Chest infections	Restrictive lung disease, NIV	-	Obstructive lung disease	-	-	-	Tracheostomy, NIV	-	-	-	NIV	NIV	-	↓FVC	↓Respiratory function	-	-
Hearing loss	-	Conductive	+	Conductive	-	-	Mild	Conductive	Conductive	-	Conductive (resolved)	-	-	-	NR	-	-	-
Speech problems	Dysarthria	Dysarthria	Dysarthria	+	-	Dysarthria	-	TY	-	-	TY	Dysarthria	TY	-	-	Nasal speech	Nasal speech	Speech delay
Malignant hyperthermia	+	-	+	+	+	-	+	+	+	-	-	-	-	-	+	+	-	+
Cryptorchidism	+	-	-	+	+	+	+	+	+	+	+	+	+	-	+	-	-	-
Other	Cervical vertebral fusion, SCD, MLD	-	-	Ventriculomegaly, HCM (resolved)	Patella AHE, stabilization, MLD, recurrent bradycardias	Mild limitation right eye abduction	-	-	-	-	-	-	-	-	-	-	-	-

<sup>a</sup>Details specified where available; “-”: not present; “+”: present; “↑”: increased; “↓”: decreased; “↗”: slow improvement; “↘”: slow deterioration; AC: Afro-Caribbean; AF: African; AHE: acute hemorrhagic encephalomyelitis; BM: birth weight; BT: bilateral talipes; CHD: congenital hip dislocation; CO: Comoro Islands; CP: cleft palate; CPAP = continuous positive airway pressure; CR = cryptorchidism; FF = finger flexion; FM = fetal movements; FVC = forced vital capacity; HCM = hypertrophic cardiomyopathy; HP: high palate; BU: bifid uvula; IUGR: intrauterine growth retardation; K: kyphosis; L: left; LL: lower limb; ME: Middle East; MLD: mild learning difficulties; MT: monolateral talipes; NIV: noninvasive ventilation; NR: not recorded; PEG: percutaneous endoscopic gastrostomy; R: right; S: scoliosis; SAm: South American; SCD: sickle cell disease; TY: too young; Ul: under investigation; UL: upper limb.

more rapidly progressive that led to early death in two of them. These patients were not available for assessment and were therefore not included in the study.

Onset was at birth in all cases. Clinical severity ranged from a more severe prenatal/neonatal onset, to a milder slowly progressive, congenital myopathy phenotype, as documented in at least three children. Polyhydramnios was recorded in three pregnancies and reduced fetal movements were noted in three additional pregnancies. The majority of the patients presented with hypotonia at birth and talipes (uni- or bilateral). Neck, elbows, wrists, fingers, or toes contractures were noted in six infants. Ten patients had cleft or high palate, one infant had a bifid uvula and an elevated right hemidiaphragm (PN5). Four infants presented with low birth weight. Feeding difficulties at birth and/or in infancy were documented in 15 patients. Eight infants had a variable degree of respiratory difficulties at birth and in the first days or life, with one (PN5) suffering severe perinatal asphyxia and cardiac arrest.

At last assessment, all patients were able to walk at least for short distances. All patients show mild to moderate, proximal more than distal upper and lower limb weakness, with axial weakness in 12 of them. Lower leg muscle atrophy was observed in 11 patients. Ptosis and facial weakness was present in all patients, while none had ophthalmoplegia. Contractures, in particular of fingers and ankles, were reported in 14 patients. Joint laxity was documented in seven patients, three of whom without associated contractures (PN6A-B-C). Scoliosis, kyphosis, and spinal rigidity were reported in 11 patients. Eight individuals showed dental malocclusion, malar hypoplasia, and jaw prominence (Figure 2). Respiratory compromise was reported in eight patients. At the time of last assessment, four children received noninvasive ventilatory support. During infancy, 13 children had failure to thrive, and six needed nasogastric tube or gastrostomy feeding. Recurrent bradycardia and ventricular hypertrophy (resolved after age 1 year) were reported in two patients. Six children had speech delay or dysarthria and seven had documented hearing loss. Seven of the 11 male patients had cryptorchidism.

### 3.2.1 | Malignant hyperthermia

Adverse reaction to anesthetics was reported in 10 patients after general anesthetics (GA). Detailed description of the full course of MH is available for patient PN5. Following five uneventful GAs, at a GA at age 6 months, because of difficult intravenous access, inhalational induction of anesthesia (with sevoflurane 8%, nitrous oxide 50%, and oxygen 50%) was carried out until successfully securing intravenous access approximately 45 min later. During this period, upper limb tone increased, end-tidal carbon dioxide increased, and attempts were made to increase minute ventilation manually. Heart rate had initially dropped from 164 bpm to 139 bpm at induction, but after 50 min induction was 208 bpm with a mean blood pressure of 53 mmHg. One hour after induction, core temperature was 39.6°C, and both upper and lower limb tone was markedly increased. Dantrolene was given and vital signs immediately improved with steady decrease in heart rate, temperature, and reduction of muscle tone. Post-event biochemistry failed to detect myoglobinuria, raise in serum creatine kinase (CK), or potassium. The highest CK levels were 69 IU/L at 14 h post event.

PN6A had CK levels of about 600 IU/L and normal myoglobin levels after the MH-like event. Normal post-event CK and myoglobin levels were documented in two further patients.

### 3.3 | Muscle MRI findings

Muscle MRI demonstrated slightly asymmetric, distal more than proximal, posterior more than anterior involvement, with semimembranosi muscles being the most affected. Asymmetric involvement of biceps femoris and semitendinosus muscles was noted in patient PN2D only (Figure 2c(iii)). In the lower legs, tibialis anterior (TA) and posterior compartment muscles were relatively preserved in patient PN1 (Figure 2c(i)), while patient PN2D showed a mild asymmetric involvement of the TA muscle (Figure 2c(iii), bottom). Asymmetric lower leg involvement, in particular of the soleus muscle, was also observed in patient PN2A (Figure 2c(ii), bottom).

### 3.4 | Histopathological features

Muscle biopsies from quadriceps from patients PN2D (taken at 9 years), PN3A (at 8 years), PN4 (at 1 year), PN5 (at 1 month), PN7 (at 2 months), and PN8 (at 3 months) showed myopathic changes (Figure 3). All biopsies showed variation in fiber size, no excess fat or connective tissue (Figure 3a,b) with predominance of type I/slow myosin fibers in most (Figure 3c-f). Although both fiber types showed variation in size, the smaller fibers were frequently type I/slow myosin fibers. Some biopsies also showed occasional fibers with internal nuclei, whorled and split fibers. Some very small fibers expressed fetal myosin, but not developmental myosin, suggesting that they were not regenerating fibers. These very small fibers expressing fetal myosin occur in a number of myopathic conditions and are currently of unknown origin (Dubowitz, Sewry, & Oldfors, 2013).

Electron microscopy analysis showed myofibrillar loss, irregular and broken Z-lines with mini-core areas with disrupted sarcomeres (Figure 3g,h). Mitochondria were of variable size, shape, and distribution. Swollen sarcoplasmic reticulum was present in some samples. The structure of triads appeared preserved, but the T-tubule component was often prominent and a little swollen.

### 3.5 | STAC3 variants affect ECC and RyR1-mediated calcium release

To investigate the functional consequences of the detected *STAC3* variants, we studied  $Ca^{2+}$  homeostasis in myotubes from *STAC3* patients. Primary myoblasts were available from patients PN2D and PN5, however, cells from patient PN2D failed to differentiate and form multinucleated myotubes so that the functional assessment of the *STAC3* variants could only be carried out on cells from patient PN5. The resting cytosolic  $[Ca^{2+}]_i$  levels, measured with the ratiometric fluorescent  $Ca^{2+}$  indicator fura-2, did not show significant differences between PN5 and control myotubes (Figure 4a), nor there were differences in the size of the intracellular  $Ca^{2+}$  stores (Figure 4b).

Next, we assessed whether myotubes from PN5 displayed differences in their dose response curves to 4-CMC and KCl-induced  $Ca^{2+}$

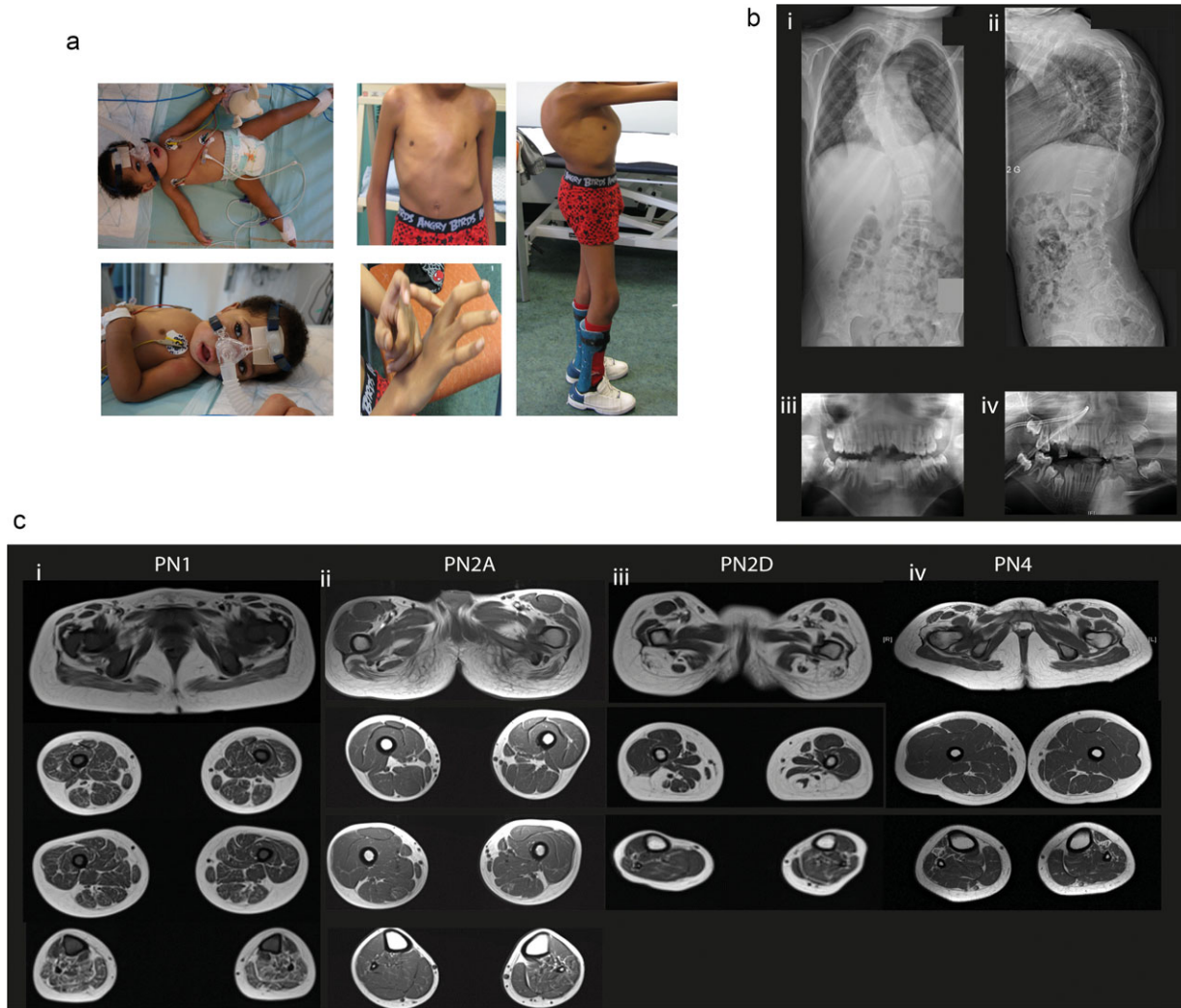


**FIGURE 2** Clinical, X-ray and muscle MRI images of patients with *STAC3* variants. (a) Clinical images of patients with *STAC3* variants. (b) Spine and orthopantomogram X-ray images of patients PN1 (age 13 years; i–iii) and PN2D (age 9 years; iv). (c) Lower limb muscle MRI of patients PN1 (age 14 years; i), PN2A (age 12 years; ii), PN2D (age 4 years; iii), and PN4 (age 21; iv)

release, a typical feature associated with the MH-susceptible phenotype due to dominant *RYR1* variants. The presence of the mutated *STAC3* did not significantly affect the  $EC_{50}$  for 4-CMC in control ( $363.7 \pm 44 \mu\text{M}$ ) and PN5 myotubes ( $384.2 \pm 30 \mu\text{M}$ ) or for KCl in control ( $10.6 \pm 0.6 \text{ mM}$ ) and PN5 myotubes ( $12.7 \pm 1.2 \text{ mM}$ ). However, the peak  $\text{Ca}^{2+}$  in response to 4-CMC was significantly reduced (Figure 4c) as was the KCl-induced  $\text{Ca}^{2+}$  release, which was reduced to approximately 10% of that observed in control myotubes (Figure 4d).

### 3.6 | Cellular localization of RyR1 and $\text{Ca}_v1.1$ in myotubes from *STAC3* patients

Confocal microscopy analysis of differentiated myotubes derived from patient PN5 and controls demonstrated no changes in the localization of RyR1 and  $\text{Ca}_v1.1$  (Figure 5a).

Similar patterns of  $\text{Ca}_v1.1$  and RyR1 distribution in patients' muscle samples compared to controls was also detected by immunohistochemical analysis showing that in *STAC3* patients  $\text{Ca}_v1.1$  and RyR1 co-localized in the muscle fibers (Figure 5b). In patient muscle

samples, intense  $\text{Ca}_v1.1$  and RyR1 staining was noted in some small fibers, which are possibly extremely atrophic fibers or fibers with fetal myosin heavy chain (MHC) expression.

### 3.7 | Effect of p.(Trp284Ser) and c.997-1G > T variants on *STAC3* protein structure

The guanine to cytosine transversion at position c.851 (c.851G > C), observed in the patients, results in a substitution of the highly conserved tryptophan (Trp) with serine (Ser). Trp284 is located in the first SH3 domain of *STAC3*. The SH3 domains have been found in signal-transducing adaptor proteins (Mayer & Baltimore, 1993) and likely serve as anchoring sites for recruitment of substrates or mediate the formation of large protein complexes (Morton & Campbell, 1994). The ligand-binding site of the SH3 domains is a hydrophobic surface with three shallow grooves formed by highly conserved aromatic residues, one of which is Trp284. These conserved aromatic residues are important for peptide binding as they establish hydrophobic interactions with key residues in the SH3-binding ligands (Lim & Richards, 1994; Zafra-Ruano & Luque, 2012).

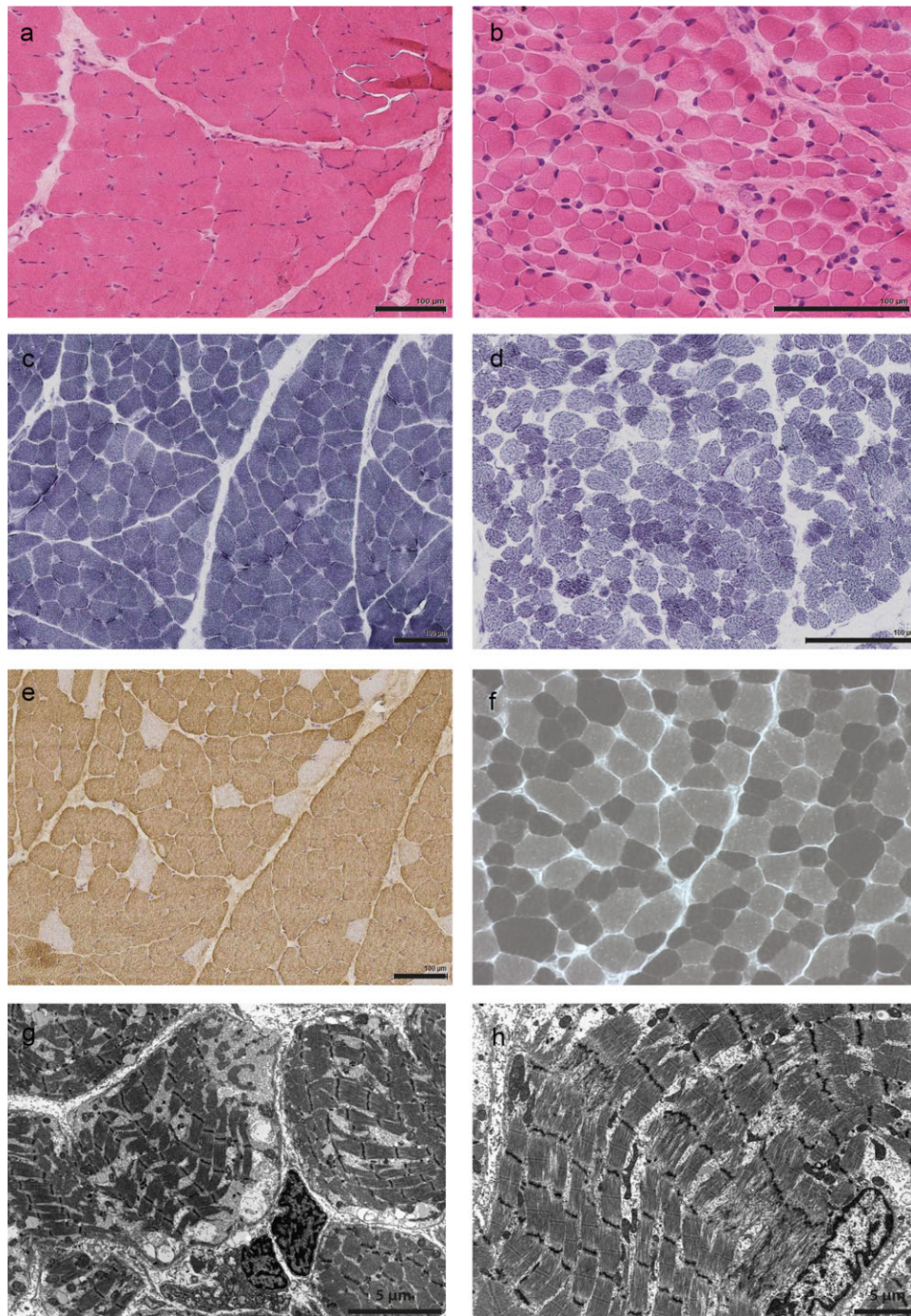


**FIGURE 3** Histological features in the STAC3 patients showing myopathic changes with variation in fiber size without excess fat or connective tissue (Hematoxylin and Eosin staining: a, b) and predominance of type I fibers (NADH-tetrazolium reductase: c, d; slow myosin: e; ATPase pH4.6: e). Scale bar 100  $\mu\text{m}$  (a, b, c, d, e). Electron microscopy revealed myofibrillar loss, swollen sarcoplasmic reticulum, irregular and broken Z-lines and sarcomere disruption, mitochondria of variable size and distribution (g, h). Scale bar 5  $\mu\text{m}$  (g, h)

To predict the effect of the substitution of Trp284 with Ser, we used the NMR structure of the first SH3 domain of STAC protein (PDB ID: 2DL4). The change of Trp to Ser side chain did not appear to lead to clashes that could disrupt packing of the STAC3 protein (Figure 6a(ii)). However, the Trp to Ser change at 284 removes the conserved aromatic residue at the surface of the ligand-binding site (Figure 6a(iii,iv)), indicating that the mutant STAC3 could have impaired protein-binding properties.

The c.997-1G > T acceptor splice site variant leads to in-frame deletion of four amino acids (Ile333-Val334-Val335-Gln336) from the second SH3 domain in STAC3. To predict the consequence of the deletion, we carried out homology modeling based on the structure of the tandem SH3 domains of human STAC1 (6B25). The data showed that the in-frame deletion affects the structure of the second SH3 domain by eliminating several  $\beta$ -strands and disturbing the five-stranded  $\beta$ -sheet (Figure 6c).

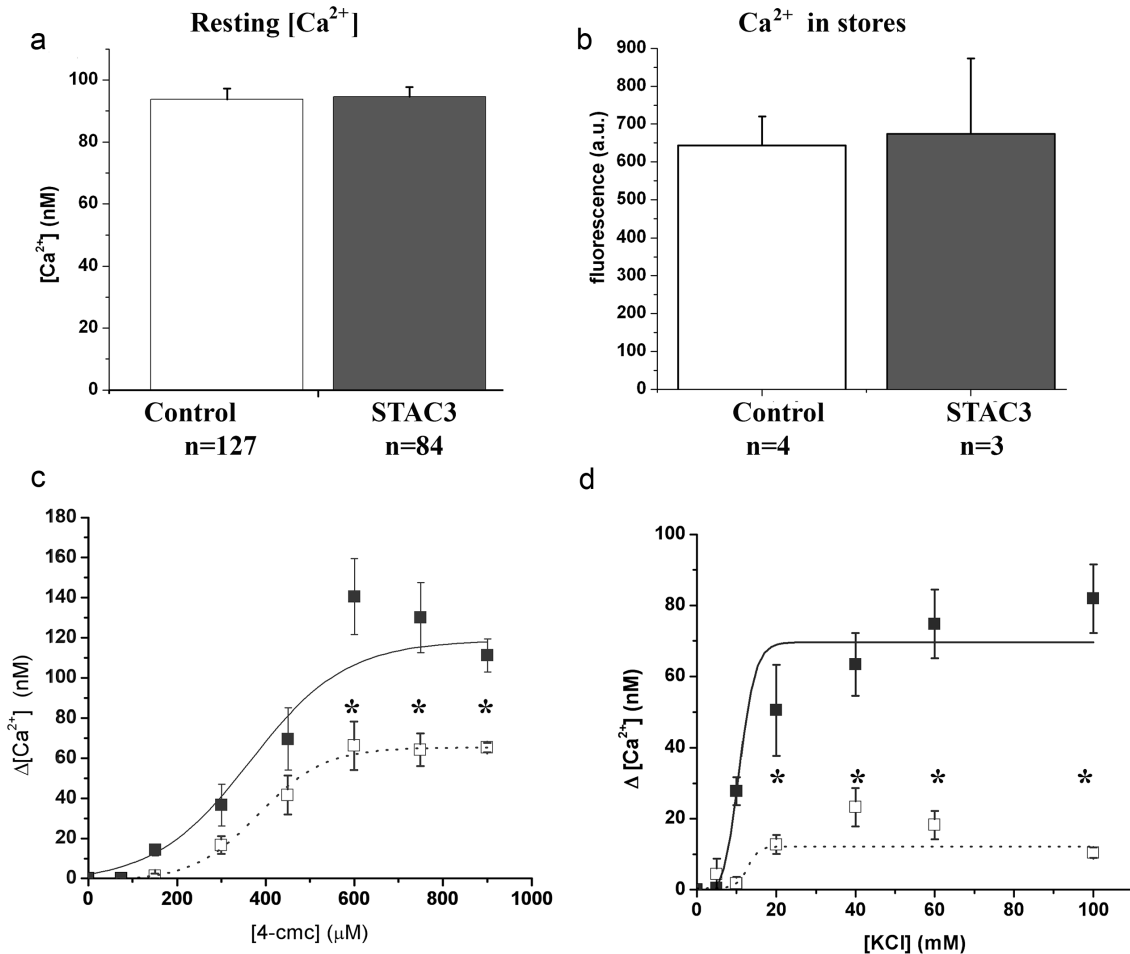


**FIGURE 4** Functional analyses of the STAC3 variants on Ca<sup>2+</sup> homeostasis and EC coupling. (a) Resting [Ca<sup>2+</sup>]<sub>i</sub> concentration, (b) size of intracellular Ca<sup>2+</sup> stores, (c) dose response to 4-CMC, and (d) dose response to KCl (peak Ca<sup>2+</sup>) in myotubes from patient PN5 (open squares) and a control (dark squares). Each symbol is the mean ( $\pm$ SEM) value of five to 10 cells. \*Corresponds to  $P < 0.01$

### 3.8 | STAC3 and Ca<sub>v</sub>1.1 interaction

We next assessed the protein expression of STAC3, Ca<sub>v</sub>1.1, and the  $\beta_{1a}$  auxiliary subunit of DHPR (DHPR- $\beta_{1a}$ ) in protein extracted from the available patient muscle tissue samples (PN2D, PN5, PN6A) and in control samples. Western blot analysis demonstrated no significant change in the content of any of the tested proteins in patient muscle samples (Figure 6b).

To determine if the p.(Trp284Ser) variant disrupts the stable interaction between STAC3 and Ca<sub>v</sub>1.1, we performed co-immunoprecipitation experiments using an anti-Ca<sub>v</sub>1.1 antibody in clarified muscle homogenates from patients PN2D, PN5, PN6A and control individuals. No difference in the apparent interaction between Ca<sub>v</sub>1.1 and the p.(Trp284Ser) STAC3 was observed as the anti-Ca<sub>v</sub>1.1 antibody pulled down STAC3 in both patient and control muscle samples (Figure 6d).

## 4 | DISCUSSION

In this study we report 18 patients of non-Native American ethnicity affected by congenital myopathy of variable severity due to recessive

STAC3 variants. In childhood, the patients at the severe end of the clinical spectrum developed progressive contractures, scoliosis, and significant feeding and respiratory difficulties. Patients with the milder form often showed improvement of respiratory and feeding difficulties with age.

A recognizable facial "Gestalt", with weakness, ptosis, downslanting palpebral fissures, downturned corners of the mouth, and high-arched and/or cleft palate, specifically guided diagnosis in four families. Weakness was predominantly axial and proximal, static, or slowly progressive. Cryptorchidism was reported in almost half of the male patients. Interestingly, a high number of patients had hearing loss (mostly conductive) and speech delay. As STAC3 is not expressed in the heart, the observation of cardiac problems in two individuals is likely to be unrelated. Long-term follow-up and description of further patients with STAC3 variants will clarify this issue.

Adverse reaction to anesthetics was common. Where detailed documentation was available, myoglobinuria, high increase in CK or potassium levels were absent and the onset of symptoms was more gradual. "Classic" MH often occurs rapidly with subsequent cardiovascular collapse and almost invariably results in post-event laboratory findings, indicating significant muscle breakdown (raised CK, urine

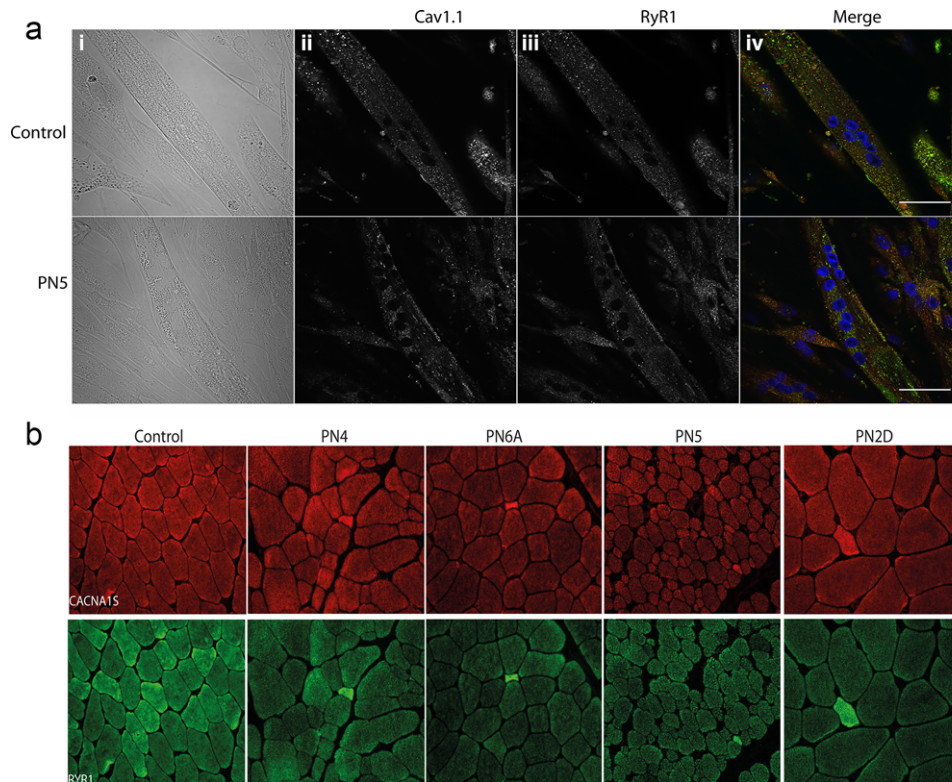


**FIGURE 5** Localization of  $Ca_v1.1$  and RyR1 in differentiated myotubes and in muscle sections from *STAC3* patients. (a) Localization of  $Ca_v1.1$  and RyR1 in myotubes from a control (top panels) and *STAC3* patient PN5 (bottom panels). Image of differentiated myotubes (panel i), anti- $Ca_v1.1$  (panel ii), anti-RyR1 (panel iii), merged image of anti- $Ca_v1.1$  (green), anti-RyR1 (red), and DAPI (blue; panel iv). Scale bar = 50  $\mu$ m. (b) Expression of  $Ca_v1.1$  and RyR1 in muscle biopsy samples from *STAC3* patients.  $Ca_v1.1$  (red) and RyR1 (green) labeling in control and in PN4, PN6A, PN5, and PN2D patients showing no significant abnormality. Fiber typing with the RyR1 antibody was visible in the control but not in the *STAC3* patients, likely due of type 1 fiber predominance. The small very brightly labeled fibers with RyR1 probably correspond to the occasional small fibers present that express fetal myosin

myoglobin, and serum potassium). The responsiveness to intravenous dantrolene and the other clinical parameters observed in our patients were suggestive of an MH-like reaction. Larger cohort of patients will be required to determine if there are consistent clinical differences between *STAC3*-related and “classical” MH and to elucidate the molecular basis of these differences.

The phenotype of this cohort overlaps with that previously reported in *STAC3* patients but also expands the clinical spectrum. We observed patients with rather severe congenital presentations, with pterygium, feeding, and respiratory complications. One patient with severe presentation (PN5) was compound heterozygous for the recurrent NAM and a novel splice site variant. Similarly, three other reported previously patients with a more severe phenotype carried variants other than the recurrent NAM variant (frameshift or splice site variants; Grzybowski et al., 2017; Telegrafi et al., 2017). However, it is worth noting that a degree of clinical variability is also observed among patients with homozygous NAM variant and among members of the same family, suggesting that factors other than the type of variants could contribute to the phenotypic variability.

The majority of the families included in this study were of known African, Afro-Caribbean, or Middle Eastern descent. The descent of the Lumbee Native American tribe is controversial, but has been speculated to include an admixture of Native Americans, European

settlers, and African Americans (Zhang et al., 2015). The observation of the NAM variant in various populations often of African descent could point toward a common ancestor of possible African origin. Interestingly, Telegrafi et al. (2017) found that the NAM variant was not in linkage with the same haplotype in their two families, implying that these variants originated from unrelated mutational events. Further studies and haplotype analysis might help to further clarify this point.

The functional analysis of the consequence of endogenously expressed *STAC3* variants were performed in patient PN5, carrying the compound heterozygous p.(Trp284Ser) and c.997-1G>T variants, inducing in-frame deletion of four amino acids from the second SH3 domain. The two SH3 domains in *STAC3* have a unique organization compared to other SH3-containing proteins; the two domains are connected through a short linker thus forming rigid interaction between the domains and an extensive interdomain interface (Wong King Yuen et al., 2017). Modeling of the in-frame deletion demonstrated that it disturbs the structure of the second *STAC3* SH3 domain, affects the hydrogen bonds between the residues, and thus likely destabilizes the structure of *STAC3* SH3 domains.

The functional data strongly support the notion that the *STAC3* variants lead to impaired ECC. Indeed, application of KCl caused a small release of sarcoplasmic reticulum  $Ca^{2+}$ , a result consistent with previous observations in animal models (Cong, Doering, Grange, &

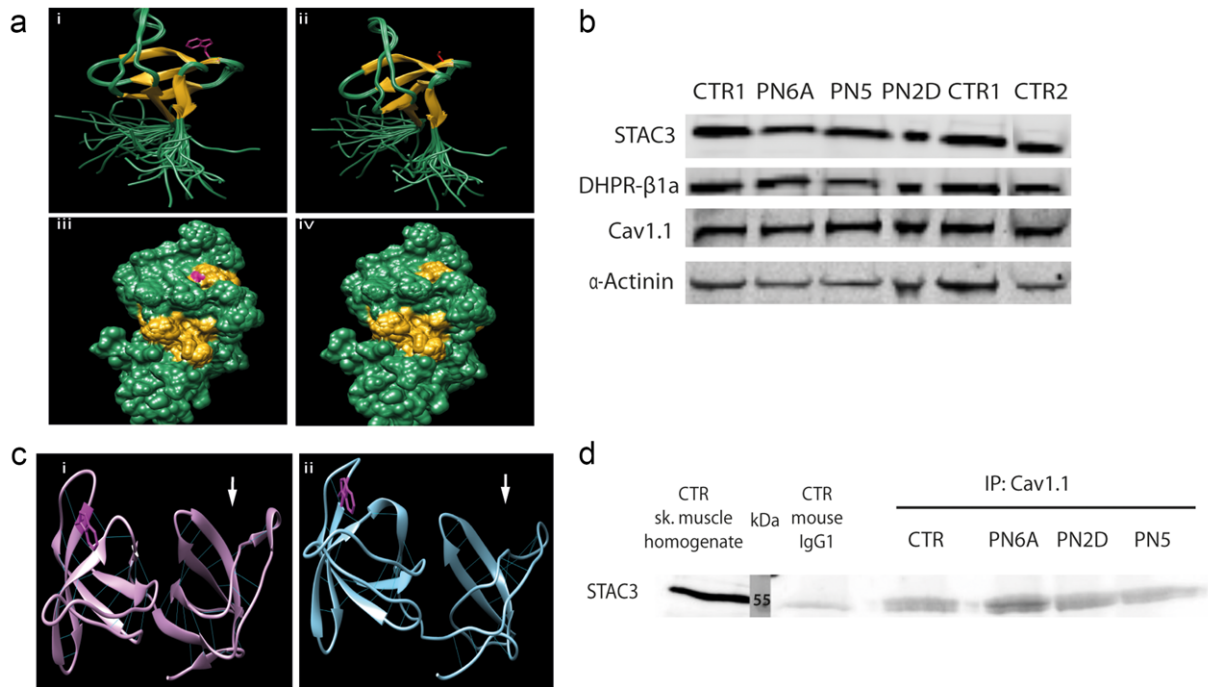


**FIGURE 6** STAC3 p.(Trp284Ser) does not affect the stable interaction with  $Ca_v1.1$ . (a) Protein model of STAC SH3 domain. Location of Trp284 (purple; i) and mutant Ser284 (red; ii) on the  $\beta$ -barrel structure of SH3 domain. Surface presentation of the wild type (iii) and mutant (iv) SH3 domain. Trp284 is presented in purple. (b) Western blot analysis of the expression of STAC3,  $Ca_v1.1$ , and DHPR- $\beta_{1a}$  in skeletal muscle samples from STAC3 patients and controls. Loading control is  $\alpha$ -actinin. (c) The homology modeling of the tandem STAC3 SH3 domain sequence carrying the in-frame deletion of four amino acids from the second SH3 domain (ii) is based on the STAC1 SH3 domains (i). The second SH3 domain is indicated with white arrows, Trp284 located in the first SH3 domain is presented with magenta and hydrogen bonds are presented as blue lines. (d) Co-immunoprecipitation of STAC3 with anti- $Ca_v1.1$  antibody in muscle samples from STAC3 patients and control

Jiang, 2016; Linsley, Hsu, Groom, et al., 2017; Nelson et al., 2013; Polster et al., 2016). Our results, however, are not fully supportive of previously published data on  $Ca^{2+}$  release mediated by direct RyR1 activators. In the PN5 myotubes, application of the direct RyR1 agonist 4-CMC (Zorzato, Scutari, Tegazzin, Clementi, & Treves, 1993) induced lower  $Ca^{2+}$  release compared to that observed in control myotubes. This is in contrast to results of Cong, Doering, Grange, et al. (2016) that demonstrated that in *Stac3*<sup>-/-</sup> mouse myotubes the peak calcium transient, induced by 5 mM 4-CMC and 25 mM caffeine, were similar to controls. It should be pointed out however, that 5 mM 4-CMC is a supramaximal concentration that may activate calcium release by RyR3 and/or other intracellular channels, which are also expressed in mouse myotubes (Ward et al., 2000). The calcium peak in response to caffeine was reportedly similar in myotubes from *stac3*<sup>-/-</sup> zebrafish and controls (Linsley, Hsu, Groom, et al., 2017; of note in the supplementary Figure 5, the peak calcium induced by caffeine is reduced by about 25%), but in *stac3*<sup>NAM</sup> fibers, the peak calcium response was significantly enhanced, with no change in the  $EC_{50}$  for caffeine. Our results in patient myotubes also showed no shift in sensitivity to either KCl or 4-CMC-mediated  $Ca^{2+}$  release in cells harboring mutant STAC3. These findings suggest that the cellular events underlying the MH-like reactions appear to be different from those underlying “classical” MH, in that (a) there is no shift in sensitivity to activating stimuli and (b) no significant increase in the resting  $[Ca^{2+}]_i$ . Nevertheless the STAC3 variants affect both depolarization-induced  $Ca^{2+}$  release as well as  $Ca^{2+}$  release triggered by direct activation of RyR1. Interestingly,

a recent study on myotubes from patients with *CACNA1S* variants, reported a decreased KCl-induced  $Ca^{2+}$  release, without altered resting  $[Ca^{2+}]_i$  or size of intracellular sarcoplasmic reticulum stores (Schartner et al., 2017). In this case, the decreased response was caused by decreased content of  $Ca_v1.1$ .

A role of STAC3 in regulating  $Ca_v1.1$  trafficking and localization to the sarcolemma has been shown (Polster et al., 2015). However, our data in STAC3 patient myotubes demonstrated that both  $Ca_v1.1$  and RyR1 were present and co-localized correctly in the patient's cells, indicating that the pathomechanism of STAC3 variants is not through impaired  $Ca_v1.1$  trafficking. The data is in agreement with studies on mouse *Stac3*<sup>NAM</sup> myotubes in which ECC was impaired without the membrane targeting of  $Ca_v1.1$  being affected (Polster et al., 2016).

As STAC3 has been shown to be a part of the DHPR complex and to stably interact with  $Ca_v1.1$  (Campiglio & Flucher, 2017; Horstick et al., 2013; Linsley, Hsu, Groom, et al., 2017), we hypothesized that the defective ECC in STAC3 patients was a result of impaired binding to  $Ca_v1.1$ . Nevertheless, co-immunoprecipitation of STAC3 with  $Ca_v1.1$  in patient and control muscle samples pulled down STAC3 to equal extent and demonstrated that the protein interaction between STAC3 and  $Ca_v1.1$  was not significantly affected by the STAC3 variants. In agreement, Campiglio and Flucher (2017) identified that the interaction between STAC3 and  $Ca_v1.1$  is through a protein-binding pocket in the C1 domain of STAC3, and the p.(Trp284Ser) variant does not impair the stable STAC3- $Ca_v1.1$  interaction. An additional STAC3- $Ca_v1.1$ -binding site has been identified in a recent study, which demon-

strated that STAC3 interacts with the  $Ca_v1.1$  linker connecting transmembrane domains II-III (Wong King Yuen et al., 2017). While the p.(Trp284Ser) variant did not cause misfolding of the STAC3 protein, it abolished the interaction with the  $Ca_v1.1$  II-III loop, which was previously identified as essential for the  $Ca_v1.1$ -RyR1 functional interaction (Grabner et al., 1999). This additional interaction could lead to loss of the functional interaction with RyR1 and possibly could explain the impaired ECC in STAC3 patients.

In conclusion, in view of our results, the recently published data describing STAC3 variants in patients of non-Native American ethnicity, and the rather homogenous clinical presentations in patients of different ethnicities, we propose to name this condition as STAC3-related congenital myopathy, to highlight its wider distribution. STAC3 gene analysis should be included in the diagnostic work up of patients of any ethnicity presenting with a congenital myopathy, in particular if a history of MH is reported. While the precise underlying pathomechanism remains to be elucidated, functional characterization of p.(Trp284Ser) in myotubes and muscle biopsy samples from STAC3 patients demonstrated that the defective ECC is not a result of  $Ca_v1.1$  sarcolemma mislocalization or impaired STAC3- $Ca_v1.1$  interaction.

## ACKNOWLEDGMENTS

The authors would like to acknowledge the support from Rachael Mein and Darren Chambers from the Dubowitz Neuromuscular Centre, UCL Institute of Child Health, London. The support of MRC Centre for Neuromuscular Diseases Biobank is acknowledged for providing patients' samples.

The research leading to these results has received funding from: the European Commission Seventh Framework Programme (FP7/2007–2013) under grant agreement no. 2012–305121 “Integrated European –omics research project for diagnosis and therapy in rare neuromuscular and neurodegenerative diseases (NEUROMICS),” the European Union's Horizon 2020 research and innovation programme under grant agreement no. 779257 “Solving the unsolved Rare Diseases (Solve-RD),” the Muscular Dystrophy Association under grant agreement MDA577346 “Novel CMD and CMY genes: Discovery and functional analysis,” the SNF (Grant number 31003A-169316), from the OPO Stiftung and NeRAB Association (to Susan Treves). The study was also supported by the NIHR Great Ormond Street Hospital Biomedical Research Centre. The views expressed are those of the author(s) and not necessarily those of the NHS, the NIHR, or the Department of Health. Work in C.G. Bönnemann's laboratory is supported by intramural funds by the National Institute for Neurological Disorders and Stroke/NIH.

## ORCID

Irina T. Zaharieva  <http://orcid.org/0000-0002-7663-6297>

## REFERENCES

- Bachmann, C., Jungbluth, H., Muntoni, F., Manzur, A. Y., Zorzato, F., & Treves, S. (2017). Cellular, biochemical and molecular changes in muscles from patients with X-linked myotubular myopathy due to MTM1 mutations. *Human Molecular Genetics*, 26(2), 320–332. <https://doi.org/10.1093/hmg/ddw388>
- Bower, N. I., de la Serrana, D. G., Cole, N. J., Hollway, G. E., Lee, H. T., Assinder, S., & Johnston, I. A. (2012). Stac3 is required for myotube formation and myogenic differentiation in vertebrate skeletal muscle. *Journal of Biological Chemistry*, 287(52), 43936–43949. <https://doi.org/10.1074/jbc.M112.361311>
- Campiglio, M., & Flucher, B. E. (2017). STAC3 stably interacts through its C1 domain with  $Ca_v1.1$  in skeletal muscle triads. *Scientific Reports*, 7, 41003. <https://doi.org/10.1038/srep41003>
- Censier, K., Urwyler, A., Zorzato, F., & Treves, S. (1998). Intracellular calcium homeostasis in human primary muscle cells from malignant hyperthermia-susceptible and normal individuals. Effect Of overexpression of recombinant wild-type and Arg163Cys mutated ryanodine receptors. *Journal of Clinical Investigation*, 101(6), 1233–1242. <https://doi.org/10.1172/jci993>
- Cong, X., Doering, J., Grange, R. W., & Jiang, H. (2016). Defective excitation-contraction coupling is partially responsible for impaired contractility in hindlimb muscles of Stac3 knockout mice. *Scientific Reports*, 6, 26194. <https://doi.org/10.1038/srep26194>
- Cong, X., Doering, J., Mazala, D. A., Chin, E. R., Grange, R. W., & Jiang, H. (2016). The SH3 and cysteine-rich domain 3 (Stac3) gene is important to growth, fiber composition, and calcium release from the sarcoplasmic reticulum in postnatal skeletal muscle. *Skeletal Muscle*, 6, 17. <https://doi.org/10.1186/s13395-016-0088-4>
- Dubowitz, V., Sewry, C. A., & Oldfors, A. (2013). *Muscle biopsy: A practical approach* (4th ed.). Philadelphia, PA: Saunders Elsevier.
- Flucher, B. E., Phillips, J. L., & Powell, J. A. (1991). Dihydropyridine receptor alpha subunits in normal and dysgenic muscle in vitro: Expression of alpha 1 is required for proper targeting and distribution of alpha 2. *Journal of Cell Biology*, 115(5), 1345–1356.
- Grabner, M., Dirksen, R. T., Suda, N., & Beam, K. G. (1999). The II-III loop of the skeletal muscle dihydropyridine receptor is responsible for the Bi-directional coupling with the ryanodine receptor. *Journal of Biological Chemistry*, 274(31), 21913–21919.
- Grzybowski, M., Schanzer, A., Pepler, A., Heller, C., Neubauer, B. A., & Hahn, A. (2017). Novel STAC3 mutations in the first non-Amerindian patient with Native American myopathy. *Neuropediatrics*, 48, 451–455. <https://doi.org/10.1055/s-0037-1601868>
- Horstick, E. J., Linsley, J. W., Dowling, J. J., Hauser, M. A., McDonald, K. K., Ashley-Koch, A., ... Kuwada, J. Y. (2013). Stac3 is a component of the excitation-contraction coupling machinery and mutated in Native American myopathy. *Nature Communications*, 4, 1952. <https://doi.org/10.1038/ncomms2952>
- Lim, W. A., & Richards, F. M. (1994). Critical residues in an SH3 domain from Sem-5 suggest a mechanism for proline-rich peptide recognition. *Nature Structural Biology*, 1(4), 221–225.
- Linsley, J. W., Hsu, I. U., Groom, L., Yarotsky, V., Lavorato, M., Horstick, E. J., ... Kuwada, J. Y. (2017). Congenital myopathy results from misregulation of a muscle  $Ca^{2+}$  channel by mutant Stac3. *Proceedings of the National Academy of Sciences of the United States of America*, 114(2), E228–E236. <https://doi.org/10.1073/pnas.1619238114>
- Linsley, J. W., Hsu, I. U., Wang, W., & Kuwada, J. Y. (2017). Transport of the alpha subunit of the voltage gated L-type calcium channel through the sarcoplasmic reticulum occurs prior to localization to triads and requires the beta subunit but not Stac3 in skeletal muscles. *Traffic*, 18(9), 622–632. <https://doi.org/10.1111/tra.12502>
- Mayer, B. J., & Baltimore, D. (1993). Signalling through SH2 and SH3 domains. *Trends in Cell Biology*, 3(1), 8–13.
- Morton, C. J., & Campbell, I. D. (1994). SH3 domains. Molecular ‘Velcro’. *Current Biology*, 4(7), 615–617.
- Nakai, J., Tanabe, T., Konno, T., Adams, B., & Beam, K. G. (1998). Localization in the II-III loop of the dihydropyridine receptor of a sequence critical for

- excitation-contraction coupling. *Journal of Biological Chemistry*, 273(39), 24983–24986.
- Nelson, B. R., Wu, F., Liu, Y., Anderson, D. M., McAnally, J., Lin, W., ... Olson, E. N. (2013). Skeletal muscle-specific T-tubule protein STAC3 mediates voltage-induced  $Ca^{2+}$  release and contractility. *Proceedings of the National Academy of Sciences of the United States of America*, 110(29), 11881–11886. <https://doi.org/10.1073/pnas.1310571110>
- Nishi, M. (1995). [Excitation-contraction uncoupling and muscular degeneration lacking functional skeletal muscle ryanodine-receptor gene]. *Tanpakushitsu Kakusan Koso*, 40(14), 2181–2187.
- Pettersen, E. F., Goddard, T. D., Huang, C. C., Couch, G. S., Greenblatt, D. M., Meng, E. C., & Ferrin, T. E. (2004). UCSF Chimera: A visualization system for exploratory research and analysis. *Journal of Computational Chemistry*, 25(13), 1605–1612. <https://doi.org/10.1002/jcc.20084>
- Polster, A., Nelson, B. R., Olson, E. N., & Beam, K. G. (2016). Stac3 has a direct role in skeletal muscle-type excitation-contraction coupling that is disrupted by a myopathy-causing mutation. *Proceedings of the National Academy of Sciences of the United States of America*, 113(39), 10986–10991. <https://doi.org/10.1073/pnas.1612441113>
- Polster, A., Nelson, B. R., Papadopoulos, S., Olson, E. N., & Beam, K. G. (2018). Stac proteins associate with the critical domain for excitation-contraction coupling in the II-III loop of CaV1.1. *Journal of General Physiology*, 150, 613–624. <https://doi.org/10.1085/jgp.201711917>
- Polster, A., Perni, S., Bichraoui, H., & Beam, K. G. (2015). Stac adaptor proteins regulate trafficking and function of muscle and neuronal L-type  $Ca^{2+}$  channels. *Proceedings of the National Academy of Sciences of the United States of America*, 112(2), 602–606. <https://doi.org/10.1073/pnas.1423113112>
- Reinholt, B. M., Ge, X., Cong, X., Gerrard, D. E., & Jiang, H. (2013). Stac3 is a novel regulator of skeletal muscle development in mice. *PLoS One*, 8(4), e62760. <https://doi.org/10.1371/journal.pone.0062760>
- Rios, E., & Pizarro, G. (1991). Voltage sensor of excitation-contraction coupling in skeletal muscle. *Physiological Reviews*, 71(3), 849–908. <https://doi.org/10.1152/physrev.1991.71.3.849>
- Sali, A., & Blundell, T. L. (1993). Comparative protein modelling by satisfaction of spatial restraints. *Journal of Molecular Biology*, 234(3), 779–815. <https://doi.org/10.1006/jmbi.1993.1626>
- Schartner, V., Romero, N. B., Donkervoort, S., Treves, S., Munot, P., Pierson, T. M., ... Laporte, J. (2017). Dihydropyridine receptor (DHPR, CACNA1S) congenital myopathy. *Acta Neuropathologica*, 133(4), 517–533. <https://doi.org/10.1007/s00401-016-1656-8>
- Stamm, D. S., Aylsworth, A. S., Stajich, J. M., Kahler, S. G., Thorne, L. B., Speer, M. C., & Powell, C. M. (2008). Native American myopathy: Congenital myopathy with cleft palate, skeletal anomalies, and susceptibility to malignant hyperthermia. *American Journal of Medical Genetics A*, 146A(14), 1832–1841. <https://doi.org/10.1002/ajmg.a.32370>
- Telegrafi, A., Webb, B. D., Robbins, S. M., Speck-Martins, C. E., Fitz-Patrick, D., Fleming, L., ... Sobreira, N. L. M. (2017). Identification of STAC3 variants in non-Native American families with overlapping features of Carey-Fineman-Ziter syndrome and Moebius syndrome. *American Journal of Medical Genetics A*, 173, 2763–2771. <https://doi.org/10.1002/ajmg.a.38375>
- Ward, C. W., Schneider, M. F., Castillo, D., Protasi, F., Wang, Y., Chen, S. R., & Allen, P. D. (2000). Expression of ryanodine receptor RyR3 produces  $Ca^{2+}$  sparks in dyspedic myotubes. *Journal of Physiology*, 525(Pt 1), 91–103.
- Wong King Yuen, S. M., Campiglio, M., Tung, C. C., Flucher, B. E., & Van Petegem, F. (2017). Structural insights into binding of STAC proteins to voltage-gated calcium channels. *Proceedings of the National Academy of Sciences of the United States of America*, 114(45), E9520–E9528. <https://doi.org/10.1073/pnas.1708852114>
- Zafra-Ruano, A., & Luque, I. (2012). Interfacial water molecules in SH3 interactions: Getting the full picture on polyproline recognition by protein-protein interaction domains. *FEBS Letters*, 586(17), 2619–2630. <https://doi.org/10.1016/j.febslet.2012.04.057>
- Zhang, C., Roque, D., Ehrisman, J. A., DiSanto, N., Broadwater, G., Doll, K. M., ... Havrilesky, L. J. (2015). Lumbee Native American ancestry and the incidence of aggressive histologic subtypes of endometrial cancer. *Gynecologic Oncology Reports*, 13, 49–52. <https://doi.org/10.1016/j.gore.2015.06.004>
- Zorzato, F., Scutari, E., Tegazzin, V., Clementi, E., & Treves, S. (1993). Chlorocresol: An activator of ryanodine receptor-mediated  $Ca^{2+}$  release. *Molecular Pharmacology*, 44(6), 1192–1201.

**How to cite this article:** Zaharieva IT, Sarkozy A, Munot P, et al. STAC3 variants cause a congenital myopathy with distinctive dysmorphic features and malignant hyperthermia susceptibility. *Human Mutation*. 2018;1–15. <https://doi.org/10.1002/humu.23635>